An RF-Ultrasound Relay for Powering Deep Implants Across Air-Tissue Interfaces with a Multi-Output Regulating Rectifier and Ultrasound Beamforming

Ernest So*, Pyungwoo Yeon*, E. J. Chichilnisky, and Amin Arbabian
Stanford University, Stanford, CA, USA, Email: soernest@stanford.edu

Abstract Single modality wireless power has limited depth for mm-sized implants across air-tissue (e.g. retina implants) or skull-tissue interfaces because of high loss in tissue (RF, optical) or high reflection at the medium interface (ultrasound). The proposed RF-ultrasound (US) relay uses an RF link across the interface to a relay chip which rectifies the RF power and transmits focused ultrasound to the implant using a 6-channel phased array with 251% efficiency improvement at 2.5 cm over fixed focusing.

Introduction Wireless powering has the potential to enable long-term, mm-sized implantable medical devices (IMDs) for sensing and stimulation. The common modalities for wireless power: RF, US, and optical either have high attenuation in tissue or a large reflection loss at the interface. RF can efficiently transmit across the interface but has high loss in tissue at depth [1, 2]. US has low tissue loss [3] but has a high loss at the interface due to the acoustic impedance mismatch of the two mediums. Finally, optical techniques suffer from high link loss from scattering in tissue outside of the eye. The RF-US relay architecture addresses these issues by utilizing RF to bypass the interface and a relay to efficiently convert the energy to US [4].

System Architecture The RF-US relay adapted to a retina implant application system diagram is shown in Fig. 1. The RF transmitter located on the glasses transmits power through the inductive link to a wearable relay which comprises a receiver coil, chip, and a piezoelectric array. The relay chip rectifies the incoming RF power (40.68 MHz) to produce three DC power supplies (1.8 V, 4.5 V, 6 to 29 V) for the US power amplifiers (PA) and control circuitry. To deliver sufficient power while avoiding excessive tissue heating, the relay power conversion efficiency (PCE) should be maximized. This is accomplished by a single power conversion stage multi-output regulating rectifier (MORR) and US beamforming with 6-channel PAs. The MORR generates a free-wheeling high-voltage (HV) and two regulated low voltages (LVs), 4.7 V and 2 V, without cascaded multi-stage power conversion losses. Two HV class-D PAs adjust the power delivered to the implant with varying voltage supply (6 to 29 V) from the HV output of the MORR. Four charge recycling adiabatic PAs (1.8 V or 4.5 V supply) boost the efficiency of driving the piezo array. Each PA channel can be programmed with a 2-bit phase code for electrical beamforming to account for variations in implant placement during surgery and tissue movements over time. The 12×12 mm^2 PZT4 array (850 kHz) comprises of 12 $2 \times 2 \times 0.4$ mm^3 air backed elements in Fig. 1 with each PA channel driving 2 elements to increase the aperture and focusing gain.

State-of-the-art regulating rectifiers [5,6] are not suitable for HV IMDs, which typically require $\gtrapprox$10 V and multiple supplies. Fig. 2 shows key operations of the MORR and its switching pulse generation circuit. The free-wheeling HV diode rectifies a peak incoming voltage stored at an L_2C_2 tank into the HV DC voltage (V_{HV} < 32 V) when *SW1* is closed. The HV rectifier powers a HV input bandgap reference and 4.5 V / 1.8 V HV input linear regulators to start operating the switching pulse generator for the low voltage current-mode regulating rectifiers with V_{SU_POR} high. The switching pulse generator controls the timing of *SW1*, *2*, and *3* pulses to be nearly aligned with the reverse peak current (i_{L2}) flowing through L_2 by pulse delay modulation (PDM) so that the isolated low-voltage node, V_{IN_CP}, can generate a voltage pulse train to charge V_{LV1} and V_{LV2} to the target regulating voltages. Once charged (4.7 V / 2 V), pulse skipping modulation (PSM) skips switching pulses for voltage regulation. PSM is adopted since switching losses for *SW1*, *2*, and *3* dominate conduction loss for light load at high switching frequency. To further reduce power loss, an integrated power switch redirects V_{DD5} of the switching pulse generator from the inefficient HV input linear regulator (PCE = V_{SU45}/V_{HV}) to a more efficient regulating rectifier (V_{LV1}).

Fig. 3 shows the adiabatic PA schematic and waveforms. Utilizing the concept of adiabatic charging, the energy stored on the capacitive part of the piezoelectric load can be redistributed onto the parallel capacitors, C_f (30 pF), and re-used to charge the load on subsequent cycles to save power. Four parallel capacitors were selected as a trade-off between increased efficiency from more capacitors and the complexity in generating the control signals. Beamforming is programmed by adding the phase code to a 2-bit accumulator, which is the input to the delay-locked loop (DLL). The DLL eliminates the need for a high frequency clock by generating 8 pulses per clock cycle for the control signals of the LV PA.

Measurement Results The 2×2.3 mm^2 chip was fabricated in a TSMC 180 nm HV BCD process. The measured start-up and power switch operations of the MORR are shown in Fig. 4a and b, respectively. The measured transients of the MORR with PSM and PDM are shown in Fig. 5. The MORR with the power switch achieves 81% PCE for RF-to-DC power conversion at V_{HV} = 10 V and 186 mW load. Fig. 6a shows beamforming compensating for distance variation in the US link from 25 - 50 mm of mineral oil to mimic tissue. The PA + US link efficiency, defined as $I_{acoustic} \times$ Rx aperture / DC chip power, for a 1.5 mm diameter needle hydrophone receiver (ONDA HNC 1500) is compared with and without beamforming. At 2.5 cm, adiabatic mode on LV PAs improves the efficiency by 42% and beamforming improves the efficiency by 251%. Fig. 7 shows the *in-vitro* experiment setup with an agar eyeball phantom and benchmarking table for mm-scale implant powering systems. To the best of our knowledge, our work is the first integrated RF-US power relay system with US beamforming, which can enable powering to deep mm-scale implants robust against distance variations and angular/horizontal misalignments.

Acknowledgements The authors thank the TSMC University Shuttle Program. This work was supported by the Lu Stanford Graduate Fellowship and Stanford Neurosciences Institute. *The first two authors equally contributed to this work.

References [1] P. Feng et al., *TBioCAS*, 12(5), 2018, pp. 1088-1099. [2] Z. Yu et al., *ISSCC*, 2020, pp. 510-512. [3] M. Ghanbari et al., *ISSCC*, 2019, pp. 284-286. [4] M. Meng et al., *TCAS-II*, 2017, pp. 1137-1141. [5] H. Gougheri et al., *ISSCC*, 2017, pp. 374-375. [6] H. Gougheri et al., *TBioCAS*, 13(5), 2019, pp. 1075-1086.

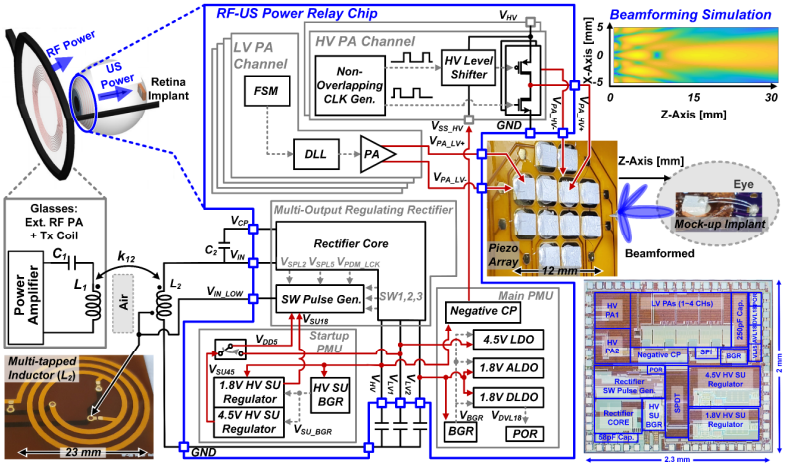

Fig. 1 System conceptual image, diagram, and chip-microphotograph.

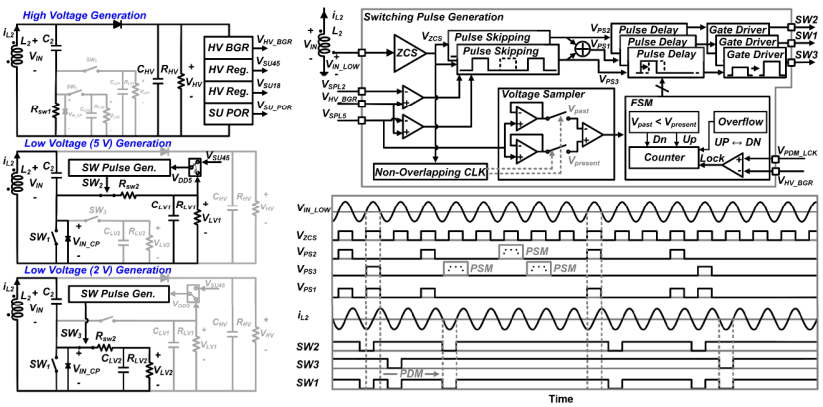

Fig. 2 Key operations of the MORR (left) and schematic diagram/key waveforms of switching pulse generation (right).

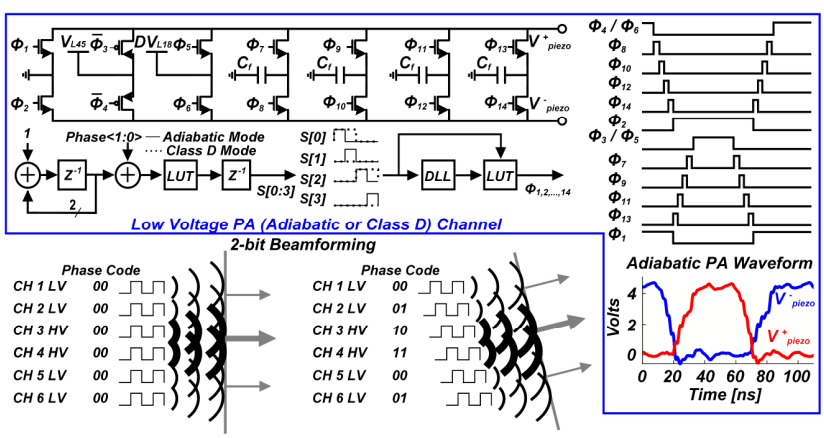

Fig. 3 Adiabatic PA schematic and operation (top), and beamforming with 2-bit phase code (bottom).

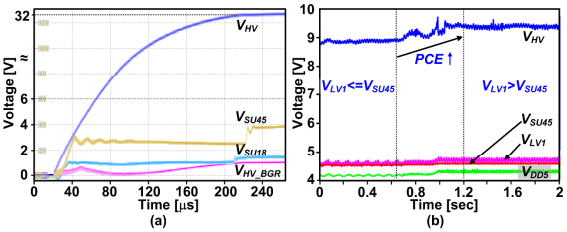

Fig. 4 Measured transient waveforms for (a) start-up and (b) power switch operations.

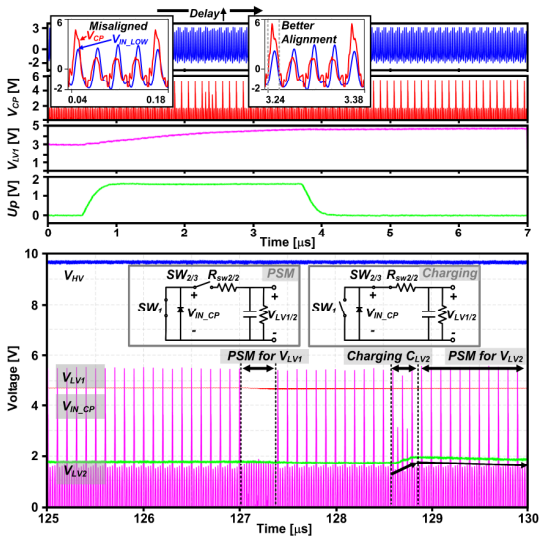

Fig. 5 Measured transient waveforms for high-voltage and low regulating voltage generation with PDM (top) and PSM (bottom).

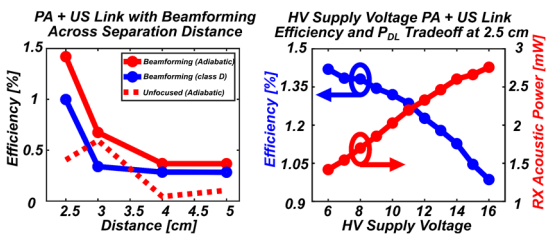

Fig. 6 PA + US link efficiency from 25 - 50 mm with beamforming shown in the left (251% improvement over unfocused at 2.5 cm). Operation of LV PAs in adiabatic mode improve the total link efficiency by 42% over class D mode at 2.5 cm as shown in the right. Trade-off between efficiency and available acoustic power at the hydrophone (2.5 cm) enabled by the tunable HV supply voltage.

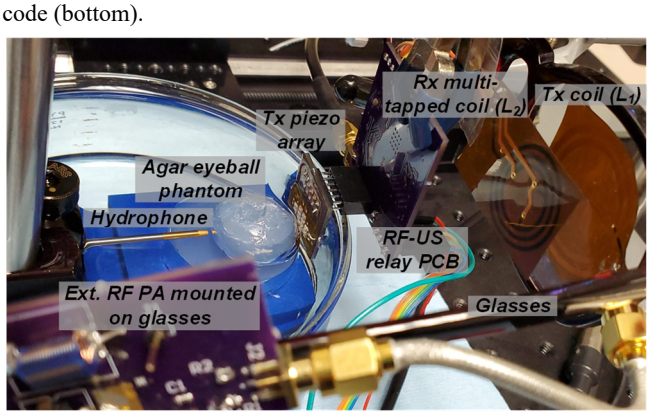

	[1] TBCAS'18	[2] ISSCC'20	[3] ISSCC'19	[4] TCAS-II'17	This Work
Power link type	2 Coil	Magnetoelectric	US	2 Coil + US	**2 Coil + US**
Including ASIC	No	Yes	Yes	No	Yes
Considers air tissue interface loss	Yes	Yes	No	Yes	Yes
Focusing	Fixed	Fixed	Fixed	Fixed	**Beamforming with 6 elements, 2 bit phase, 3 amplitude levels**
Distance [mm] (medium)	12 (Lamb rib)	0 - 30 (Saline)	40 (oil)	30 (air) + 30 (castor oil)	12 (air) + 29 (Agar eye phantom immersed in mineral oil)
PDL [mW]	-	0.39 - 0.16	0.0288	- (VNA meas.)	**0.946 (acoustic)**
Transmitter Aperture	17.2 mm diameter	25 mm diameter	25.4 mm diameter	100 mm diameter	32 mm diameter
Receiver Aperture	4 × 4 mm²	4 × 2 mm²	0.56 mm²	1.1 mm diameter	1.5 mm diameter
Efficiency[%]	PTE: 3.05	PTE × PCE: 0.08 - 0.008	-	Total link PTE:0.16	**Total end-to-end system efficiency : 0.27***
				RF link: 26 / US link: 0.66	**RF link: 86 Rectifier PCE: 81† / US PA PCE + US link: 0.86‡**

* **Total end-to-end efficiency: efficiency from DC power of the PA on the glasses to Rx acoustic power**
† **Measured when V_{HV} = 10 V** ‡**DC supply power of the US PA to acoustic power at the hydrophone**

Fig. 7 Measurement setup (left) and benchmarking of the RF-ultrasound power relay chip with state-of-the-art powering modalities (right).